Inertia Emulation in Multiterminal HVDC Networks

Alessio Clerici, Simone Negri, Enrico Tironi
Department of Electronics, Information and Bioengineering (DEIB)
Politecnico di Milano
Milan, Italy
simone.negri@polimi.it

***Abstract*— In this paper the supporting action of a multi-terminal HVDC network to one AC grid is investigated. A three-terminal HVDC network is considered, which is connected to three independent AC networks by means of a Master converter and two Slave converters. The Master converter controls the DC link voltage, while the Slave converters are controlled to exchange a predetermined power. A derivative Inertia Emulation Control (INEC) algorithm is proposed for the Master converter, allowing it to both control DC voltage and limit the AC grid ROCOF (Rate Of Change Of Frequency). Two possible solutions to improve the control effectiveness in limiting frequency deviation are considered, namely further DC link capacitors oversizing and introduction of a P-V droop characteristic on one Slave converter. Simulation results are presented to substantiate the proposed control effectiveness.**

***Index Terms*—INEC, multi-terminal HVDC, virtual inertia**

I. INTRODUCTION

High Voltage DC (HVDC) is a consolidated solution for long-distance or submarine power transmission. It is commonly known that HVDC links among between AC grids have a decoupling effect which allows asynchronous functioning of the two grids both during transients and steady-state conditions.

The application of suitable controls to the HVDC converters enables the regulation of the exchanged power between the two AC grids. The usage of thyristor-based converters, typical of higher power applications, requires the connection to active grids capable of fulfilling the converters reactive power requirements. On the contrary, IGBT-based converters, which are getting more and more widespread for HVDC applications, behave as generators capable of providing predetermined values of voltage and frequency. When connecting active grids, this allows one station to control the DC voltage, while the other one can exchange a defined power with the AC grid, potentially participating in frequency regulation. In the meantime, each converter can independently exchange a predetermined reactive power.

A more recent trend in HVDC applications introduces further functionalities in IGBT-based converters. One of the most interesting functions which can be realized by means of IGBT based conversion stations is inertia emulation [1]-[4], which is particularly useful whenever the HVDC network is connected to relatively weak grids. Some works define inertia emulation algorithms which relate the exchanged power with the frequency and its derivative, which is then applied to an HVDC station [5]-[8]. While this approach effectively contributes to stabilize grid frequency, it has two main drawbacks: firstly, it transfers the disturbance to one grid to another, even though smoothed by the converters time constants and DC link capacitors. This can be a significant issue when power scheduling is required, which is common in HVDC applications. Furthermore, being it based on the control of the exchanged power, it cannot be implemented on Master converters, but only on Slaves. In order to address this issues, generic Inertia Emulation Control (INEC) algorithms have been proposed [9]: this kind of algorithms relates DC voltage with grid frequency [9]-[11], leading to easier integration in multi-terminal HVDC. Furthermore, this approach allows to effectively exploit the DC-link capacitors as energy storage, allowing to totally or partially decouple the different AC grids connected to the multi-terminal HVDC. Consequently, INEC algorithms require a significant oversizing of the DC-link capacitors; furthermore, due to the lack of a derivative action, their response is relatively slow.

In this paper the possible supporting action of a multi-terminal HVDC network to one AC grid is investigated. A three-terminal HVDC network is considered, which is connected to three independent AC networks by means of a Master converter and two Slave converters. The Master converter controls the DC link voltage, while the Slave converters are controlled to exchange a predetermined power. A derivative INEC algorithm is proposed for the Master converter, allowing it to both control DC voltage and support grid frequency. The two Slave converters are controlled to exchange a predefined power; in particular, one is controlled to exchange a fixed power, while for the other one the introduction of a P-V droop characteristic is considered, such that it supports the master converter action.

The paper is organized as follows: Section II reports the considered multi-terminal HVDC network and converter functionalities, Section III introduces the derivative INEC control, Section IV presents simulation results and Section V draws some conclusions.

II. CONSIDERED MULTI-TERMINAL HVDC NETWORK

The considered multi-terminal HVDC network is reported in Fig. 1. It consists of a three terminal DC network with three IGBT based conversion stations, each one connected to an independent AC grid. The main data regarding HVDC conversion stations and AC grids are reported in Table 1 and Table 2, respectively, while the line parameters are reported in Table 3. HVDC stations are assumed to be able to withstand overloading conditions for a limited time [12]. HVDC station 1 is assumed to be the Master station, controlling the DC link voltage, while the other two station are assumed to be Slaves, controlling the exchanged power. The Master converter is equipped with an INEC algorithm, which will be developed in detail in Section III, such that it can support grid frequency providing virtual inertia. In the meantime, the INEC algorithm allows the Master converter to control the DC link voltage, such that the DC-link capacitors can be exploited as storages to provide the energy necessary for inertia emulation. HVDC station 2 is assumed to be a Slave converter and two subcases are investigated, namely constant power operation and operation according to a P-V droop characteristic, such that it can support the Master converter regulating action. HVDC station 3 is assumed to be a Slave converter operated at fixed power. Note that both grid 1 and grid 2 are relatively weak high-voltage grid. This is necessary not only to show the effectiveness of the proposed derivative INEC algorithm in mitigating the frequency disturbances affecting grid 1, but also to evaluate the effects on grid 2 frequency of the introduction of the droop characteristic in HVDC station 2 control, which would be insignificant in case of a strong grid.

III. INERTIA EMULATION ALGORITHM

INEC algorithms introduce a relation between AC grid frequency and DC link voltage considering the synchronous generator mechanical equations and capacitors constitutive relation. In order to clarify the reasons leading to the proposal of a derivative INEC algorithm, it is firstly useful to introduce a generic INEC algorithm. Considering firstly a basic system constituted by an equivalent synchronous generator feeding a load: neglecting the rotating loads dynamics, the relation between exchanged power and frequency is given by

$$P_E - P_L = 2H_G f_G(0)\frac{d\Delta f_G(t)}{dt} \tag{1}$$

where P_E is the electrical power supplied by the equivalent generator, P_L is the power absorbed by the load, H_G is the equivalent generator inertial coefficient, f_G is the equivalent generator frequency. Powers and frequency are expressed in pu, where the base quantities used for pu conversion are HVDC station 1 rated power (A_n) and AC grid 1 rated frequency (f_{Gn}). As mentioned, the point of INEC algorithms is getting a similar response from a static converter, exploiting

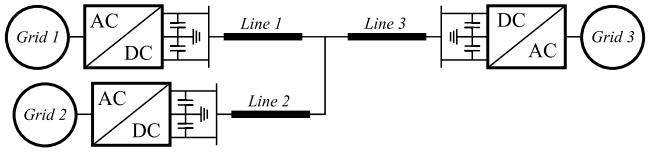

Figure 1 – Considered multi-terminal HVDC network

TABLE 1 – HVDC STATIONS DATA

	Station 1	*Station 2*	*Station 3*
Rated Power (A_n)	200 MVA	200 MVA	200 MVA
Rated DC Voltage (V_{DCn})	200 kV	200 kV	200 kV

TABLE 2 – AC GRIDS DATA

	AC Grid 1	*AC Grid 2*	*AC Grid 3*
Rated Power (A_{Gn})	2000 MVA	2000 MVA	20000 MVA
Rated Voltage (V_{Gn})	230 kV	230 kV	230 kV
Rated frequency (f_{Gn})	50 Hz	50 Hz	50 Hz
Inertial coefficient (H_G)	4 s	4 s	20 s

TABLE 3 – LINES DATA

	Line 1	*Line 2*	*Line 3*
Resistance per unit length [Ω/km]	$1.39\cdot10^{-2}$	$1.39\cdot10^{-2}$	$1.39\cdot10^{-2}$
Inductance per unit length [H/km]	$1.59\cdot10^{-4}$	$1.59\cdot10^{-4}$	$1.59\cdot10^{-4}$
Capacitance per unit length [F/km]	$2.31\cdot10^{-7}$	$2.31\cdot10^{-7}$	$2.31\cdot10^{-7}$
Line length [km]	37.5	37.5	75

the filter capacitors stored energy by means of a suitable voltage reference. In order to relate the DC voltage reference with the grid frequency, let us assume that the power corresponding to the second term of (1) is completely obtained from the discharge of the converter filter capacitors, which leads to

$$2H_V f_G(0)\frac{d\Delta f_G(t)}{dt} = \frac{C_{DC}V_{DC}(t)}{A_n}\frac{dV_{DC}(t)}{dt} \tag{2}$$

where H_V is the virtual inertial coefficient, C_{DC} is the converter DC link capacitance, V_{DC} is the the DC link voltage, expressed in pu with refrence to its rated value (V_{DCn}), and A_n is the converter rated power expressed in pu. It is worth pointing out that the virtual inertial coefficient H_V, appearing in (2), represents the inertial coefficient of the mechanical system the algorithm is emulating, while H_G, appearing in (1), is the inertial coefficient of the equivalent synchronous generator representing grid 1; the two quantities have been used for the algorithm definition, but, from here on, they are not strictly related and H_V is just a control parameter. The integration of (2) leads to

$$V_{DC}(t) = \sqrt{V_{DC}^2(0) + \frac{4H_V A_n}{V_{DCn}^2 C_{DC}}\Delta f_G(t)} \tag{3}$$

where V_{DCn} is the rated DC link voltage. Hence, (3) should guarantee that the HVDC station converter responds to a frequency disturbance similarly to a synchronous generator characterized by an inertial coefficient H_V, being the necessary energy obtained by changing the DC link voltage to exploit the DC link capacitors as storage devices. This control approach exhibits some significant advantages over classic inertia emulation: it can be implemented on the master node of a DC network, it does not require frequency derivative measurement and it does not generate conflicts with voltage regulation and its limits. On the other side, it introduces some significant drawbacks too: it is nonlinear, which requires careful evaluation of its dynamic and stability, its

effectiveness depends on voltage regulators performances and, due to the absence of a derivative term, it is not very effective in the very beginning of frequency transients (it limits maximum frequency deviation if the DC link capacitors are large enough, but is less effective on ROCOF). Furthermore, the variation of the DC link voltage affects all the converters, such that the operating conditions of each station are modified, which can affect the system efficiency; however, since the proposed control effects are limited to transients, this last issue can be considered a minor one in most cases.

In order to address the aforementioned issues, a derivative INEC algorithm is introduced. The global approach is very similar to standard INEC, but (2) is modified to include a term proportional to the second derivative of frequency by means of a suitable constant K_f, namely

$$2H_V f_G(0)\frac{d\Delta f_G(t)}{dt} = \frac{C_{DC}V_{DC}(t)}{A_n}\frac{dV_{DC}(t)}{dt}\left(1+K_f\frac{d^2\Delta f_G(t)}{dt^2}\right) \quad (4)$$

This is useful in that the second derivative of frequency, which is directly proportional to the second derivative of the mechanical angular speed, is maximum at the very beginning of transients, when the INEC action must be fast to reduce ROCOF, and almost negligible during the remaining portion of the transient, where standard INEC algorithms have proven to be an effective solution. The integration of (4), under the assumption of constant voltage derivative (which is reasonable during the very beginning of the transient) and neglecting frequency derivative in the calculation of the integration constant, leads to

$$V_{DC}(t) = \sqrt{V_{DC}^2(0) + \frac{4H_V A_n}{V_{DCn}^2 C_{DC}}\Delta f_G(t) + K_{Id}\frac{d\Delta f_G(t)}{dt}} \quad (5)$$

where $K_{Id} = K_f K_V$ and K_V is the approximated constant value of frequency derivative. Even though (5) requires a measurement of frequency derivative, it maintains all the other advantages typical of INEC algorithms, while introducing a faster response in the very beginning of transients. The application of (5) requires a significant oversizing of the DC link capacitors to provide the energy necessary to perform the inertia emulation action. A possible approach to define the necessary capacitance is

$$C_{DC} = \frac{2\cdot k_P \cdot A_n \cdot t_C}{V_{DCn}^2(1-\Delta V_{DC}^2)} \quad (6)$$

where k_P is the portion of the converter rated power A_n available for frequency regulation and inertia emulation, t_C is the time during which the capacitors are required to provide the aforementioned power and ΔV_{DC} is the maximum allowed variation of the DC voltage. According to (6), the DC link capacitors are chosen such that they can provide a predetermined active power (equal to the product of the constant k_P and the converter rated power A_n) for a certain time t_C reducing their voltage of a relative quantity ΔV_{DC}.

TABLE 4 – SIMULATION PARAMETERS

	Station 1	*Station 2*	*Station 3*
Steady-state exchanged power	0.9 *pu*	-0.35 *pu*	-0.45 *pu*
DC link capacitance	42 *mF (84 mF for the fifth simulation)*	70 *μF*	70 *μF*
Equivalent inertial coefficient (H_V)	2 *s*	-	-
Derivative action constant (K_{Id})	4 *s*	-	-
Droop coefficient	0	0.04 (last simulation only, 0 otherwise)	0

Please note that (6) is a first sizing attempt based on simple energetic considerations and it does not imply that the converter is effectively operated in the specified conditions; other approaches for capacitors sizing have been developed in [8]. Furthermore, it is worth pointing out that the main goal of this paper is not the definition of optimal sizing criteria.

IV. SIMULATION RESULTS

Simulations have been performed to evaluate the impact of the proposed HVDC stations control on frequency transients under different HVDC station 2 operating conditions. For these purposes, the total load connected to grid 1 is suddenly increased at *t=2 s*; assuming the stations rated power as base power for pu calculation, the load increase used to test the inertia emulation algorithm is equal to 0.8 pu (160 MW). The main data not yet provided and used for simulations, including the pre-existent load-flow, are reported in Table 4, where, for each HVDC station, the exchanged power is considered positive when absorbed from the AC grid. Note that, in steady state, grid 1 is providing a certain amount of power which is absorbed by grid 2 and grid 3. This implies that one of the weaker grids is feeding the stronger one; however, this is not uncommon since weaker grids often include larger amount of distributed generation and renewable energy sources, which contributes to their reduced inertia. Furthermore, note that the proposed control, analogously to the similar ones presented in the literature, is intended to mitigate the effect of abrupt transients, while it is assumed that the involved grids are capable of fulfilling the steady-state power flow before and after the transient. Thus, the steady-state load flow inside the HVDC network is the same at the end of the transient and initial conditions are non-significant as long as the power limitations of the converters are not reached during transients. However, considering that the converter can withstand overload conditions for a limited time, power capability is a minor issue. Two sets of simulations have been performed: the first one is intended to evaluate the benefits of derivative INEC with respect to standard INEC, while the second one is intended to show the effect of introducing a P-V droop characteristic on one Slave converter with respect to a further DC link capacitors oversizing.

The first set of simulation is constituted by three cases: in the first one, all converters are operated at fixed power, while in the second one a standard, non-derivative INEC algorithm has been implemented on HVDC station 1, being the other two converters still operated at fixed power. In the third

simulation, a derivative INEC algorithm has been implemented on HVDC station 1, while the other two converters are again operated at fixed power. The DC link capacitors connected to the master converter have been chosen according to (6) with $k_P = 0.4$, $t_C = 2\ s$ and $\Delta V_{DC} = 0.9$, which leads to $C_{DC} = 42\ mF$. The subsequent frequency transient in grid 1 is reported in Fig. 2; the DC link voltage measured at HVDC station 1 is reported in Fig. 3, while the active power exchanged with grid 1 is reported in Fig. 4. Considering Fig. 2, one can notice that the standard INEC algorithm reduces the frequency disturbance amplitude, but is not very effective in reducing the ROCOF: in fact, the frequency derivative at the very beginning of the transient in case of fixed power control and standard INEC is almost identical. The introduction of derivative INEC can effectively mitigate the impact of abrupt load changes on frequency but, due to the need to avoid excessive oversizing of the DC link capacitors, its effect is limited to the first three seconds: after that, the DC voltage has reached its lower limit and the control cannot continue its action. This results in a second frequency disturbance, which, even though small, is visible in Fig. 2, slightly before t=5 s. In fact, it is commonly known that capacitors are storage devices suitable to act as energy buffers due to their high specific power, but are not suitable for longer term application. With no support from other HVDC converters, the derivative INEC is effective in reducing the ROCOF, but is not very effective in reducing the maximum frequency deviation.

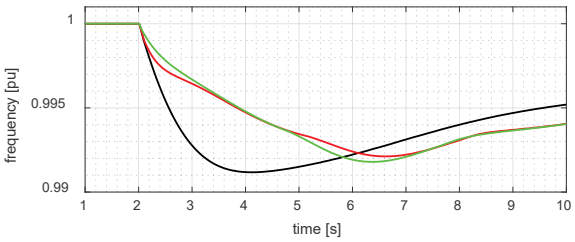

Figure 2 – Grid 1 frequency transient in case of: no INEC (black), standard INEC (red), derivative INEC (green).

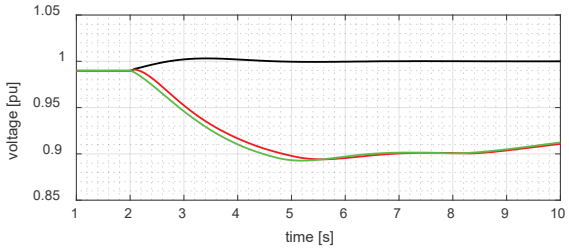

Figure 3 – DC link voltage at grid 1 terminals in case of: no INEC (black), standard INEC (red), derivative INEC (green).

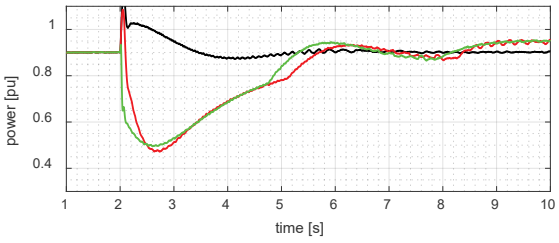

Figure 4 – Grid 1 AC power in case of: no INEC (black), standard INEC (red), derivative INEC (green).

The second set of simulation is again constituted by three cases: the first one, as in the third case of the previous set, a derivative INEC algorithm has been implemented on HVDC station 1, while the other two converters are again operated at fixed power. The second and the third cases are aimed to test possible solution to improve the proposed control effectiveness while mitigating the secondary frequency disturbance generated when the DC voltage reference reaches its lower limit: in particular, in the second case the DC link capacitor sizing has been doubled, while in the third one a P-V droop characteristic has been implemented on HVDC station 2. The subsequent frequency transient in grid 1 and grid 2 are reported in Fig. 5 and Fig. 6, respectively. The DC link voltage measured at HVDC station 1 is reported in Fig. 7, while grid 1 and grid 2 exchanged power are reported in Fig. 8 and Fig. 9, respectively. Considering the frequency profiles reported in Fig. 5 and Fig. 6, one can notice that both the doubling of the DC link capacitors and the introduction of the droop characteristic allows to avoid the frequency disturbance due to the DC link voltage reference reaching its limit. However, the introduction of the droop characteristic allows to obtain significant better performances in terms of grid 1 frequency control: the ROCOF, as expected, is the same in both situations, since it is only related to the response of the converter regulator, but the droop control allows to obtain the power needed to reduce frequency deviation. On the other hand, a small but significant disturbance is introduced in grid 2, which would not have been involved in frequency transients otherwise. Considering now the power profiles reported in Fig. 8 and Fig. 9, one can notice that both the DC link capacitors doubling and the introduction of the droop characteristic have a significant smoothing effect on the power exchanged by HVDC station 1, since the voltage reference does not reach its saturation, and consequently the aforementioned second frequency disturbance generated by the DC link voltage reaching its operational limit is avoided.

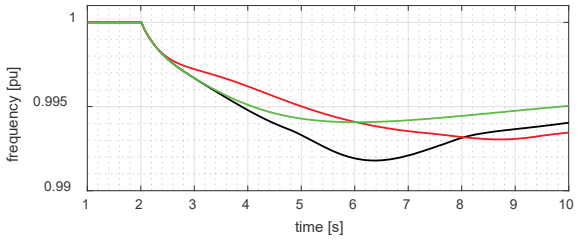

Figure 5 – Grid 1 frequency transient in case of: derivative INEC (black), derivative INEC with doubled DC link capacitors(red), derivative INEC with 4% droop on grid 2 (green).

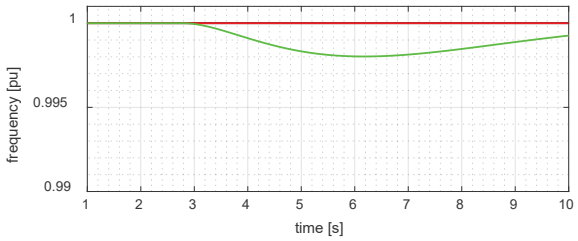

Figure 6 – Grid 2 frequency transient in case of: derivative INEC (black), derivative INEC with doubled DC link capacitors(red), derivative INEC with 4% droop on grid 2 (green).

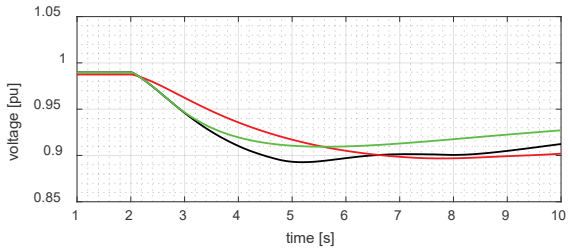

Figure 7 – DC link voltage at grid 1 terminals in case of: derivative INEC (black), derivative INEC with doubled DC link capacitors(red), derivative INEC with 4% droop on grid 2 (green).

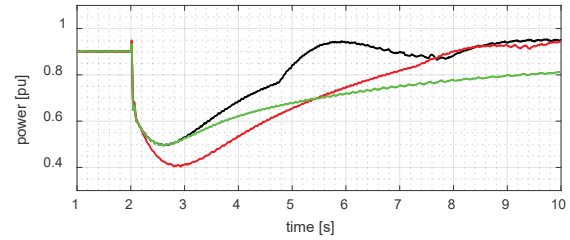

Figure 8 – Grid 1 AC power in case of: derivative INEC (black), derivative INEC with doubled DC link capacitors(red), derivative INEC with 4% droop on grid 2 (green).

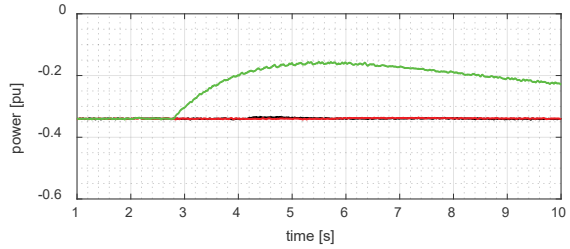

Figure 9 – Grid 2 AC power in case of derivative INEC (black), derivative INEC with doubled DC link capacitors(red), derivative INEC with 4% droop on grid 2 (green).

Grid 2 is also involved in the response to the disturbance on grid 1, but with a very smooth power profile which does not introduce large frequency disturbances in grid 2.

V. CONCLUSIONS

In this paper the possible supporting action of HVDC multi-terminal networks to the AC grid is investigated. A three terminal HVDC grid is considered and a derivative INEC control is introduced for the to mitigate the classical drawbacks of INEC algorithms. Simulation results lead to few considerations. Firstly, as expected, the introduction of the derivative terms in INEC algorithms allows to significantly improve the control effectiveness in the very beginning of the transient, which allows to reduce ROCOF, but has no significant effect on maximum frequency deviation. Furthermore, the limited possible oversizing of the DC link capacitors leads to a secondary (smaller) frequency disturbance when the voltage reference reaches its limit value and the converter must stop its regulating action. Two possible approaches to address these issues have been investigated, namely further capacitors oversizing and introduction of a P-V droop on a slave converter. The presented results suggest that, when possible, it is advisable to use a droop control to support the derivative INEC algorithm due to the smoother dynamics obtained and the reduction in frequency deviation. Even though further studies, considering in detail technical and economic aspects, are necessary to define the optimal capacitors sizing, the presented results prove that the oversizing of the DC link capacitors coupled with a derivative INEC algorithm is very effective in reducing ROCOF. Furthermore, it is suggested that the introduction of a P-V droop on a Slave converter is the best solution to address the issues related with INEC-style controls and to support primary regulation. Finally, it is worth pointing out that the Master converter voltage regulator requires particular consideration, since its performances are critical when INEC algorithms are realized.

REFERENCES

[1] N. Soni, S. Doolla and M. C. Chandorkar, "Improvement of Transient Response in Microgrids Using Virtual Inertia," in *IEEE Transactions on Power Delivery*, vol. 28, no. 3, pp. 1830-1838, July 2013.

[2] N. Soni, S. Doolla and M. C. Chandorkar, "Inertia Design Methods for Islanded Microgrids Having Static and Rotating Energy Sources," in *IEEE Transactions on Industry Applications*, vol. 52, no. 6, pp. 5165-5174, Nov.-Dec. 2016.

[3] E. Rakhshani and P. Rodriguez, "Inertia Emulation in AC/DC Interconnected Power Systems Using Derivative Technique Considering Frequency Measurement Effects," in *IEEE Transactions on Power Systems*, vol. 32, no. 5, pp. 3338-3351, Sept. 2017.

[4] S. Negri, E. Tironi and D. S. Danna, "Integrated Control Strategy for Islanded Operation in Smart Grids: Virtual Inertia and Ancillary Services," in *IEEE Transactions on Industry Applications*, vol. 55, no. 3, pp. 2401-2411, May-June 2019.

[5] L. M. Castro and E. Acha, "On the Provision of Frequency Regulation in Low Inertia AC Grids Using HVDC Systems," in *IEEE Transactions on Smart Grid*, vol. 7, no. 6, pp. 2680-2690, Nov. 2016.

[6] Y. Cao *et al*., "A Virtual Synchronous Generator Control Strategy for VSC-MTDC Systems," in *IEEE Transactions on Energy Conversion*, vol. 33, no. 2, pp. 750-761, June 2018.

[7] W. Wang, Y. Li, Y. Cao, U. Häger and C. Rehtanz, "Adaptive Droop Control of VSC-MTDC System for Frequency Support and Power Sharing," in *IEEE Transactions on Power Systems*, vol. 33, no. 2, pp. 1264-1274, March 2018.

[8] R. Chiumeo, C. Gandolfi, A. Clerici, F. C. Dezza and R. Zuelli, "Contribution of HVDC Systems in Increasing the Electrical Network Inertia: A Case Study," *2018 IEEE International Conference on Environment and Electrical Engineering and 2018 IEEE Industrial and Commercial Power Systems Europe (EEEIC / I&CPS Europe)*, Palermo, 2018, pp. 1-6.

[9] J. Zhu, J. M. Guerrero, W. Hung, C. D. Booth and G. P. Adam, "Generic inertia emulation controller for multi-terminal voltage-source-converter high voltage direct current systems," in *IET Renewable Power Generation*, vol. 8, no. 7, pp. 740-748, September 2014.

[10] H. Liu and Z. Chen, "Contribution of VSC-HVDC to Frequency Regulation of Power Systems With Offshore Wind Generation," in *IEEE Transactions on Energy Conversion*, vol. 30, no. 3, pp. 918-926, Sept. 2015.

[11] X. Liu and A. Lindemann, "Control of VSC-HVDC Connected Offshore Windfarms for Providing Synthetic Inertia," in *IEEE Journal of Emerging and Selected Topics in Power Electronics*, vol. 6, no. 3, pp. 1407-1417, Sept. 2018.

[12] I. M. Sanz, P. D. Judge, C. E. Spallarossa, B. Chaudhuri and T. C. Green, "Dynamic Overload Capability of VSC HVDC Interconnections for Frequency Support," in *IEEE Transactions on Energy Conversion*, vol. 32, no. 4, pp. 1544-1553, Dec. 2017.